

# Transverse Relaxation-Optimized Spectroscopy (TROSY) for NMR Studies of Aromatic Spin Systems in $^{13}\text{C}$ -Labeled Proteins

Konstantin Pervushin, Roland Riek, Gerhard Wider, and Kurt Wüthrich\*

Contribution from the Institut für Molekularbiologie und Biophysik Eidgenössische Technische Hochschule Hönggerberg, CH-8093 Zürich, Switzerland

Received March 5, 1998

**Abstract:** Transverse relaxation-optimized spectroscopy (TROSY) yields greatly improved sensitivity for multidimensional NMR experiments with aromatic spin systems in proteins. TROSY makes use of the fact that due to the large anisotropy of the  $^{13}\text{C}$  chemical shift tensor, the transverse relaxation of one component of the  $^{13}\text{C}$  doublet in aromatic  $^{13}\text{C}$ – $^1\text{H}$  moieties is reduced by interference of dipole–dipole (DD) coupling and chemical shift anisotropy (CSA) relaxation. The full advantage of TROSY for studies of aromatic spin systems is obtained at presently available resonance frequencies from 500 to 800 MHz. Since the  $^{13}\text{C}$  chemical shifts are recorded using a constant-time evolution period, the TROSY improvement in signal-to-noise relative to corresponding conventional NMR experiments increases with increasing molecular size and can be further significantly enhanced by combined use of the  $^1\text{H}$  and  $^{13}\text{C}$  steady-state magnetizations. With selective observation of the slowly relaxing component of the  $^{13}\text{C}$  doublets in experiments recorded without  $^1\text{H}$  decoupling during the  $^{13}\text{C}$  chemical shift evolution period, a 4–10-fold sensitivity gain for individual aromatic  $^{13}\text{C}$ – $^1\text{H}$  correlation peaks was achieved for the uniformly  $^{13}\text{C}$ -labeled 18 kDa protein cyclophilin A. A new 3D ct-TROSY-HCCH-COSY experiment is presented, which correlates the resonances of  $^{13}\text{C}$  nuclei with those of covalently bound  $^{13}\text{C}$ – $^1\text{H}$  groups and can be applied for complete identification of aromatic spin systems. In this scheme the chemical shift evolution of neighboring aromatic  $^{13}\text{C}$  spins are recorded in two indirectly detected spectral dimensions, so that the additional third dimension is obtained without increase of the number of delays.

## Introduction

Mutual compensation of different spin interactions, which individually result in rapid transverse relaxation of nuclear magnetic resonances (NMR),<sup>1</sup> has recently been used to improve both the spectral resolution and the sensitivity for observation of  $^{15}\text{N}$ – $^1\text{H}$  groups in large proteins. Here, the principles of transverse relaxation-optimized spectroscopy (TROSY)<sup>2</sup> are applied in new experiments with greatly improved sensitivity for investigations of the aromatic amino acid residues in uniformly  $^{13}\text{C}$ -labeled proteins. In NMR studies of proteins in the size range above about 10 kDa, where uniform  $^{13}\text{C}$  labeling is routinely used, the assignment of the aromatic spin systems, which are of critical importance for high quality of a structure determination,<sup>3</sup> is a severe bottleneck.<sup>4–7</sup> The presently described TROSY experiments promise to greatly improve this situation.

In aromatic spin systems the relaxation mechanisms of interest are  $^{13}\text{C}$ – $^1\text{H}$  dipole–dipole coupling (DD) and  $^{13}\text{C}$  chemical shift anisotropy (CSA) relaxation. To achieve maximally reduced relaxation, the potentially competing interactions must be comparable in magnitude.<sup>2,8</sup> Large values of the principal elements and favorable orientation of the  $^{13}\text{C}$  chemical shift tensor in aromatic groups allow effective compensation of  $^{13}\text{C}$ – $^1\text{H}$  coupling by CSA relaxation at the presently available  $^1\text{H}$  resonance frequencies of 600–800 MHz. In contrast, the small CSA values for aromatic protons make the use of the TROSY method unattractive for these nuclei. Therefore, for aromatic  $^{13}\text{C}$ – $^1\text{H}$  groups carbon chemical shifts are recorded with the TROSY method, which reduces  $^{13}\text{C}$  transverse relaxation during the  $^{13}\text{C}$  shift evolution periods, whereas broad-band  $^{13}\text{C}$  decoupling is applied during  $^1\text{H}$  signal acquisition.

The  $^{13}\text{C}$ – $^1\text{H}$  heteronuclear NMR experiments of interest for studies of aromatic spin systems in uniformly  $^{13}\text{C}$ -labeled proteins use constant-time (ct) evolution periods to eliminate homonuclear  $^{13}\text{C}$ – $^{13}\text{C}$  couplings in the  $^{13}\text{C}$  dimensions.<sup>9</sup> Transverse relaxation during constant-time periods is a major source of sensitivity loss in these [ $^{13}\text{C}$ , $^1\text{H}$ ]-correlation experiments.<sup>10</sup> Therefore, much effort was invested to reduce transverse

\* To whom correspondence should be addressed. Telephone: +41-1-6332473. FAX: +41-1-6331151.

(1) Abbreviations: NMR, nuclear magnetic resonance; rf, radio frequency; 2D, two-dimensional; 3D, three-dimensional; FID, free induction decay; DD, dipole–dipole; CSA, chemical shift anisotropy; COSY, correlation spectroscopy; TROSY, transverse relaxation-optimized spectroscopy; PFG, pulsed field gradient; hPrP(121–231), C-terminal domain of the human prion protein, residues 121–231; ct, constant-time chemical shift evolution; S/N, signal-to-noise ratio.

(2) Pervushin, K.; Riek, R.; Wider, G.; Wüthrich, K. *Proc. Natl. Acad. Sci. U.S.A.* **1997**, *94*, 12366–12371.

(3) Wüthrich, K. *NMR of Proteins and Nucleic Acids*; Wiley: New York, 1986.

(4) Wagner, G.; Brühwiler, D.; Wüthrich, K. *J. Mol. Biol.* **1987**, *196*, 227–231.

(5) Vuister, G. W.; Kim, S. J.; Wu, C.; Bax, A. *J. Am. Chem. Soc.* **1994**, *116*, 9206–9210.

(6) Grzesiek, S.; Bax, A. *J. Biomol. NMR* **1995**, *6*, 335–339.

(7) Zerbe, O.; Szyperski, T.; Ottiger, M.; Wüthrich, K. *J. Biomol. NMR* **1996**, *7*, 99–106.

(8) Goldman, M. J. *Magn. Reson.* **1984**, *60*, 437–452. Tycko, R., Ed. *Understanding Chemical Reactivity: Nuclear Magnetic Resonance Probes of Molecular Dynamics*; Kluwer Academic Publishers: Boston, 1994. Werbelow, L. G. In *Encyclopedia of NMR*; Grant, D. M.; Harris, R. K., Eds.; Wiley: New York, 1996; Vol. 6, pp 4072–4078. Dayie, K. T.; Wagner, G. *J. Am. Chem. Soc.* **1997**, *119*, 7797–7806.

(9) Vuister, G. W.; Bax, A. *J. Magn. Reson.* **1992**, *98*, 428–435.

(10) Ikura, M.; Kay, L. E.; Bax, A. *J. Biomol. NMR* **1991**, *1*, 299–304.

relaxation, mainly with the use of  $^{13}\text{C}$ - $^1\text{H}$  heteronuclear multiple-quantum coherence (HMQC) during the indirect evolution periods.<sup>6,7,11</sup> For aromatic groups, sensitivity enhancements of up to about 20% relative to the basic experiments were thus obtained for uniformly  $^{13}\text{C}$ -labeled proteins.<sup>7</sup> Since in the TROSY-type experiments only one component of the  $^{13}\text{C}$  doublet is selectively observed, it becomes possible to combine the  $^1\text{H}$  and  $^{13}\text{C}$  steady-state magnetizations in such a way that the sensitivity of the experiment is enhanced about 2-fold. Overall, we demonstrate in this paper for the 2D ct-TROSY- $^{13}\text{C}$ - $^1\text{H}$ -COSY and 3D ct-TROSY-(H)CCH-COSY experiments with  $^{13}\text{C}$ -labeled proteins of size 14–18 kDa that the sensitivity gain with TROSY is 4–10-fold for individual aromatic rings, depending on the degree of immobilization in the protein molecule.

## Methods

Aromatic  $^{13}\text{C}$ - $^1\text{H}$  groups have favorable chemical shift anisotropy (CSA) for the implementation of TROSY-type NMR experiments.<sup>2</sup> For a carbon spin in a six-membered aromatic ring the most highly shielded direction,  $\sigma_{33}$ , is perpendicular to the plane of the ring, and the least-shielded orientation,  $\sigma_{11}$ , is directed approximately along the  $^{13}\text{C}$ - $^1\text{H}$  bond,<sup>12</sup> with average values of  $\sigma_{11} = 225$  ppm,  $\sigma_{22} = 149$  ppm, and  $\sigma_{33} = 15$  ppm. In TROSY experiments these large values and the favorable orientation of the  $^{13}\text{C}$  CSA tensor in aromatic  $^{13}\text{C}$ - $^1\text{H}$  groups provide efficient compensation of  $^{13}\text{C}$ - $^1\text{H}$  dipolar coupling relaxation during the  $^{13}\text{C}$  chemical shift evolution times. In contrast, the small CSA values measured for aromatic protons advise against the use of the TROSY method during proton chemical shift evolution periods. Therefore, only the aromatic carbon chemical shifts are recorded with the TROSY method, with the use of a constant-time evolution period to eliminate resonance overlap due to  $^1J(^{13}\text{C}, ^{13}\text{C})$  couplings,<sup>9</sup> whereas broadband  $^{13}\text{C}$ -decoupling is applied during proton signal acquisition. With this strategy the advantage of TROSY-type experiments will be in improved sensitivity, whereas, in contrast to the situation with  $^{15}\text{N}$ - $^1\text{H}$  groups,<sup>2</sup> the resonance line shapes and hence the spectral resolution will not be affected.

Pulse schemes for 2D ct-TROSY- $^{13}\text{C}$ - $^1\text{H}$ -COSY and 3D ct-TROSY-(H)CCH-COSY experiments are shown in Figure 1a,b. The relevant magnetization transfer steps are described by the single-transition basis operators  $S^{12}$  and  $S^{34}$ ,<sup>13</sup> which refer to the transitions  $1 \rightarrow 2$  and  $3 \rightarrow 4$  in the standard energy-level diagram for a system of two spins  $1/2$ .<sup>14</sup> The corresponding resonance frequencies are  $\omega_S^{12} = \omega_S + \pi J_{IS}$  and  $\omega_S^{34} = \omega_S - \pi J_{IS}$ , with transverse  $^{13}\text{C}$  relaxation rates  $R_{12} = \rho^* + \lambda + \eta$  and  $R_{34} = \rho^* + \lambda - \eta$ , where  $\lambda$  is the autorelaxation from  $^{13}\text{C}$ - $^1\text{H}$  dipolar coupling of the isolated  $^{13}\text{C}$ - $^1\text{H}$  fragment and  $^{13}\text{C}$  CSA,  $\eta$  is the  $^{13}\text{C}$  CSA and  $^{13}\text{C}$ - $^1\text{H}$  dipolar coupling cross-correlated relaxation, and  $\rho^*$  comprises the contributions from all other relaxation pathways. For a rigid, isotropically tumbling

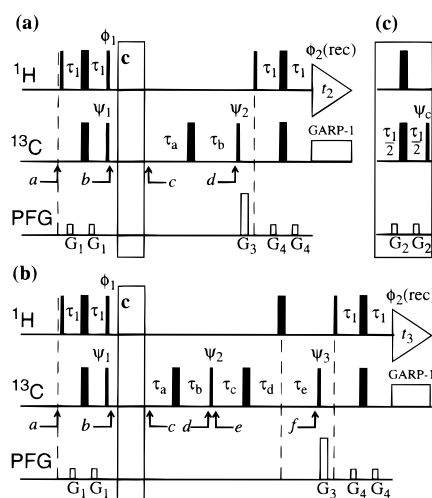


**Figure 1.** Pulse schemes of TROSY-type 2D and 3D ct- $^1\text{H}$ ,  $^{13}\text{C}$ -correlation experiments for studies of the aromatic spin systems of Tyr, Phe, Trp and His, which are optimized for minimal transverse carbon relaxation during the chemical shift evolution periods.<sup>2</sup> In each of the schemes (a–c) narrow and wide bars on the horizontal lines marked  $^1\text{H}$  and  $^{13}\text{C}$  stand for nonselective  $90^\circ$  and  $180^\circ$  rf pulses, respectively. The  $^1\text{H}$  and  $^{13}\text{C}$  carrier frequencies are placed at 4.8 and 127 ppm, respectively. The row marked PFG indicates the applied magnetic field gradients along the  $z$  axis:  $G_1 = 10$  G/cm, duration 0.8 ms;  $G_2 = 12$  G/cm, 0.8 ms;  $G_3 = 40$  G/cm, 1 ms;  $G_4 = 10$  G/cm, 0.8 ms. (a) 2D ct-TROSY- $^{13}\text{C}$ - $^1\text{H}$ -COSY, which correlates the resonances of aromatic  $^{13}\text{C}$  spins with those of the directly attached protons. The delays are  $\tau_1 = 1.6$  ms;  $\tau_a = (T - \tau_1 + t_1)/2$ ;  $\tau_b = (T - \tau_1 - t_1)/2$ . The duration of the constant-time period,  $T$ , is set to  $1/{}^1J_{CC} = 17.6$  ms. The rf pulse phases are set to  $x$  except when indicated otherwise:  $\psi_1 = \{\pi/4, 5\pi/4\}$ ;  $\psi_c = \{x\}$ ;  $\psi_2 = \{2(x), 2(-x)\}$ ;  $\phi_1 = \{-y\}$ ;  $\phi_2(\text{receiver}) = \{x, -x, -x, x\}$ . Quadrature detection in the  $t_1$  dimension is obtained by applying the States-TPPI technique<sup>20</sup> with the phase  $\psi_2$ . (b) 3D ct-TROSY-(H)CCH-COSY, which correlates the resonances of  $^{13}\text{C}$  spins with those of the directly bound  $^{13}\text{C}$ - $^1\text{H}$  moieties in aromatic rings. The delays are  $\tau_1 = 1.6$  ms;  $\tau_a = 6.6\text{ms} + t_1/2$ ;  $\tau_b = 6.6\text{ms} - t_1/2$ ;  $\tau_c = 2.2\text{ms} - t_2/2$ ;  $\tau_d = 0.6\text{ms}$ ;  $\tau_e = 1.6\text{ms} + t_2/2$ . The two constant-time delays,  $T_a = \tau_a + \tau_b$  and  $T_b = \tau_c + \tau_d + \tau_e$ , were set to  $3/(4{}^1J_{CC})$  and  $1/(4{}^1J_{CC})$ , respectively. The phase cycling scheme used was  $\psi_1 = \{\pi/4, 5\pi/4\}$ ,  $\psi_c = \{x\}$ ,  $\psi_2 = \{2(y), 2(-y)\}$ ,  $\psi_3 = \{x\}$ ,  $\phi_1 = \{-y\}$ ,  $\phi_2(\text{receiver}) = \{x, -x, -x, x\}$ . Quadrature detection in the  $t_1$  dimension is obtained using States-TPPI<sup>20</sup> by simultaneously incrementing each of the phases  $\psi_1$  and  $\psi_c$  by  $90^\circ$ , and in  $t_3$  by applying States-TPPI with  $\psi_3$ . (c) Insert similar to a  $S^3E$  element,<sup>17</sup> which is used to suppress the fast-relaxing component of the  $^{13}\text{C}$  doublet is typically attenuated beyond detection by fast transverse relaxation (see text). If c is not used, the phase  $\phi_1 = \{x\}$  in both experiments. In this paper we also use a 2D version of the experiment (b), which is obtained by setting  $t_2 = 0$  (Figure 2d). The arrows labeled a to d in a and a to f in b identify time points discussed in the text.

spherical molecule the  $^{13}\text{C}$  autorelaxation rate,  $\lambda$ , and the interference term,  $\eta$ , are given by the eqs 1 and 2:<sup>8</sup>

$$\lambda = (p + \delta_S)\{4J(0) + 3J(\omega_S)\} + \delta_S \{J(\omega_I - \omega_S) + 3J(\omega_I) + 6J(\omega_I + \omega_S)\} \quad (1)$$

$$\eta = (K_1 + K_2)\{4J(0) + 3J(\omega_S)\} \quad (2)$$

$\omega_S$  and  $\omega_I$  are the Larmor frequencies of the spins  $S$  and  $I$ . The coupling constants are defined as  $p = 1/8(\gamma_I\gamma_S\hbar/r_{IS}^3)^2$ ,  $\delta_S = 1/18(\omega_S\Delta\sigma_S)^2$ , and  $K_i = 1/6\gamma_I\gamma_S\hbar\omega_S\Delta_i(3\cos^2(\Phi_i) - 1)/2r_{IS}^3$ , where  $\gamma_I$  and  $\gamma_S$  are the gyromagnetic ratios of  $I$  and  $S$ ,  $\hbar$  is the Planck constant divided by  $2\pi$ ,  $r_{IS}$  is the distance between the nuclei  $S$  and  $I$ ,  $(\Delta\sigma_S)^2 = \Delta_1^2 + \Delta_2^2 - \Delta_1\Delta_2$ , with  $\Delta_1 = \sigma_{33} - \sigma_{11}$

(11) Griffey, R. H.; Redfield, A. G. *Q. Rev. Biophys.* **1987**, *19*, 51–82. Grzesiek, S.; Kuboniwa, H.; Hinck, A. P.; Bax, A. *J. Am. Chem. Soc.* **1995**, *117*, 5312–5315. Marino, J. P.; Diener, J. L.; Moore, P. B.; Griesinger, C. *J. Am. Chem. Soc.* **1997**, *119*, 7361–7366. Yamazaki, T.; Tochio, H.; Furui, J.; Aimoto, S.; Kyogoku, Y. *J. Am. Chem. Soc.* **1997**, *119*, 872–880. Swapna, G. V. T.; Rios, C. B.; Shang, Z.; Montelione, G. T. *J. Biomol. NMR* **1997**, *9*, 105–111. Shang, Z.; Swapna, G. V. T.; Rios, C. B.; Montelione, G. T. *J. Am. Chem. Soc.* **1997**, *119*, 9274–9278.

(12) Veeman, W. S. *Prog. NMR Spectrosc.* **1984**, *16*, 193–235.

(13) Ernst, R. R.; Bodenhausen, G.; Wokaun, A. *The Principles of Nuclear Magnetic Resonance in One and Two Dimensions*; Clarendon Press: Oxford, 1987. Sørensen, O. W.; Eich, G. W.; Levitt, M. H.; Bodenhausen, G.; Ernst, R. R. *Prog. NMR Spectrosc.* **1983**, *16*, 163–192.

(14) Farrar, T. C.; Stringfellow, T. C. In *Encyclopedia of NMR*; Grant, D. M., Harris, R. K., Eds.; Wiley: New York, 1996; Vol. 6, 4101–4107.

and  $\Delta_2 = \sigma_{22} - \sigma_{11}$ , and  $\Phi_i$  is the angle between the internuclear vector  $I-S$  and the principal direction of the chemical shift tensor. In the following product operator description of the experiment an explicit treatment of the spin-spin relaxation is given for the chemical shift evolution periods, but in the interest of clarity of the representation, relaxation during polarization transfers and during the signal acquisition periods is not considered. The spin operators used are  $I_1, I_2$ , and  $I_3$  for protons, and  $S_1, S_2$ , and  $S_3$  for the respective directly attached  $^{13}\text{C}$  nuclei.

The improvement in sensitivity of TROSY-type experiments is based on recording the  $^{13}\text{C}$  chemical shifts using the  $S_x^{34}$  magnetization only, which corresponds to the component of the  $^{13}\text{C}$  doublet with the smaller transverse relaxation rate,  $R_{34}$ . In the conventional reference experiments,<sup>9,10</sup> proton decoupling during  $^{13}\text{C}$  evolution periods results in the effective relaxation rate  $R_2 = 1/2(R_{12} + R_{34}) = \rho^* + \lambda$ , which is significantly faster than  $R_{34}$  in the situation typically encountered in larger proteins. In  $^{13}\text{C}$  constant-time experiments this difference in the transverse relaxation rates translates into a significant improvement of the signal-to-noise ratio ( $S/N$ ), since the signal amplitude is proportional to  $\exp(-R_2T)$ , where  $T$  is the duration of the ct period and  $R_2$  is the transverse relaxation rate. In addition, TROSY provides the possibility of further improving the sensitivity by combined use of the  $^1\text{H}$  and  $^{13}\text{C}$  steady-state magnetizations,<sup>2</sup> which is not accessible with the conventional NMR techniques. In the following product operator analysis of TROSY-type experiments with  $^{13}\text{C}-^1\text{H}$  moieties we first describe the combined use of the  $^1\text{H}$  and  $^{13}\text{C}$  steady-state magnetizations and then discuss the relevant relaxation factors. A quantitative analysis of the relative contributions to improved sensitivity from transverse relaxation optimization and from the use of the  $^{13}\text{C}$  steady-state magnetization is given in the Discussion section.

In the ct-TROSY- $^{13}\text{C}, ^1\text{H}$ -COSY experiment, the longitudinal magnetizations of the nuclei  $I$  and  $S$  at time  $a$  (Figure 1a) can be described as

$$\sigma_a = uI_{1z} + vS_{1z} \quad (3)$$

where the constant factors  $u$  and  $v$  reflect the relative magnitudes of the steady-state proton and carbon magnetizations, respectively, which are determined by the spin-lattice relaxation rates and the duration of the delay between data recordings.<sup>13</sup> At time  $b$ , considering the  $\pi/4$  phase shift of the  $\psi_1$  pulse, the density operator is given by

$$\sigma_b = \frac{1}{\sqrt{2}}[(u2I_{1z}S_{1y} + vS_{1y}) - (u2I_{1z}S_{1x} + vS_{1x})] \quad (4)$$

The density operator  $\sigma_b$  can be expressed by eq 7 when considering that the magnetization of the individual components of the  $S$  doublet can be described using the single-transition basis operators  $S_i^{12}$  and  $S_i^{34}$ ,

$$S_i^{12} = \frac{1}{2}S_i + I_zS_i, \quad i = x, y \quad (5)$$

$$S_i^{34} = \frac{1}{2}S_i - I_zS_i, \quad i = x, y \quad (6)$$

$$\sigma_b = \frac{1}{\sqrt{2}}[(u+v)(S_{1y}^{12} - S_{1x}^{12}) - (u-v)(S_{1y}^{34} - S_{1x}^{34})] \quad (7)$$

Equation 7 then shows that the  $^{13}\text{C}$  steady-state magnetization contributes to the polarization of one transition and reduces

polarization of the other one. To achieve complete suppression of the resulting "minor" transition, the element of Figure 1c is inserted between time points  $b$  and  $c$ , resulting in the density operator of eq 8 at time  $c$ :

$$\sigma_c = (u-v)S_{1z}^{12} + (u+v)S_{1x}^{34} \quad (8)$$

Since the  $S_{1z}^{12}$  operator does not evolve during  $t_1$ , only the magnetization of the  $S_x^{34}$  component of the  $S$  multiplet then needs to be further considered.

The time evolution of the single-transition operator  $S_x^{34}$  during  $t_1$  can be described by a product of the spin operator with trigonometric coefficients and a monoexponential function representing relaxation,<sup>2</sup> so that at time  $d$

$$\sigma_d = -(u+v) \cos^2(\pi^1J_{CC}T) \sin(\omega_{1S}^{34}t_1) S_{1y}^{34} \exp(-R_{34}T) \quad (9)$$

In eq 9 operators which are not converted back to observable proton magnetization have been omitted. With the ct period  $T = 1/J_{CC}$ , the magnetization observed during the acquisition period  $t_2$  is

$$\sigma_t = ((u+v)/2) I_{1x} \sin(\omega_{1S}^{34}t_1) \exp(-R_{34}T) \quad (10)$$

In eq 10 the factor  $1/2$  accounts for the fact that only one component of the  $^{13}\text{C}$  doublet is observed. The cosine-modulated signal is obtained by application of the pulse sequence with the phase  $\psi_2$  incremented by  $90^\circ$ .

In the 3D ct-TROSY-(H)CCH-COSY experiment (Figure 1b) the evolution of magnetization can be described using eqs 1–8, resulting in the observable proton magnetization at time  $d$  as given by

$$\sigma_d = -(u+v) \cos^2(\pi^1J_{CC}T_a) \sin(\omega_{1S}^{34}t_1) S_{1y}^{34} \times \exp(-R_{34}T_a) + (u+v) \sin(\pi^1J_{CC}T_a) \cos(\pi^1J_{CC}T_a) \times \sin(\omega_{1S}^{34}t_1) (2S_{2z}S_{1x}^{34} + 2S_{3z}S_{1x}^{34}) \exp(-R_{34}T_a) \quad (11)$$

The two terms in eq 11 represent, respectively, the direct peaks and the relay peaks in the  $\omega_1$  dimension. After the evolution between the time points  $e$  and  $f$ , the magnetization of interest is given by

$$\sigma_f = -\cos^2(\pi^1J_{CC}T_b) \cos(\omega_{1S}t_2) 2I_{1z}S_{1y} \exp(-R_2T_b) + \sin(\pi^1J_{CC}T_b) \cos(\pi^1J_{CC}T_b) [\cos(\omega_{2S}t_2) 2I_{2z}S_{2x} + \cos(\omega_{3S}t_2) 2I_{3z}S_{3x}] \exp(-R_2T_b) \quad (12)$$

For clarity the multiplicative factors (eq 11) have been omitted in eq 12 and the single-transition operators have been transformed back to the product operators. Because the second constant-time period,  $T_b = \tau_c + \tau_d + \tau_e$ , is very short (4.4 ms), it is advantageous to record the chemical shifts of the carbons  $S_1, S_2$ , and  $S_3$  with proton decoupling by a  $180^\circ(^1\text{H})$  pulse (Figure 1b), so that they are modulated by  $\omega_{1S}, \omega_{2S}$ , and  $\omega_{3S}$ , respectively. Finally, with  $T_a = 3/(4^1J_{CC})$  and  $T_b = 1/(4^1J_{CC})$  the magnetization observed during the acquisition period  $t_3$  is given by

$$\sigma_{t_3} = -((u+v)/8) I_{1x} \sin(\omega_{1S}^{34}t_1) \cos(\omega_{1S}t_2) \exp(-R_{34}T_a - R_2T_b) + ((u+v)/8) \sin(\omega_{1S}^{34}t_1) [I_{2x} \cos(\omega_{2S}t_2) + I_{3x} \cos(\omega_{3S}t_2)] \exp(-R_{34}T_a - R_2T_b) \quad (13)$$

The two terms in eq 13 represent the direct peaks and the relay

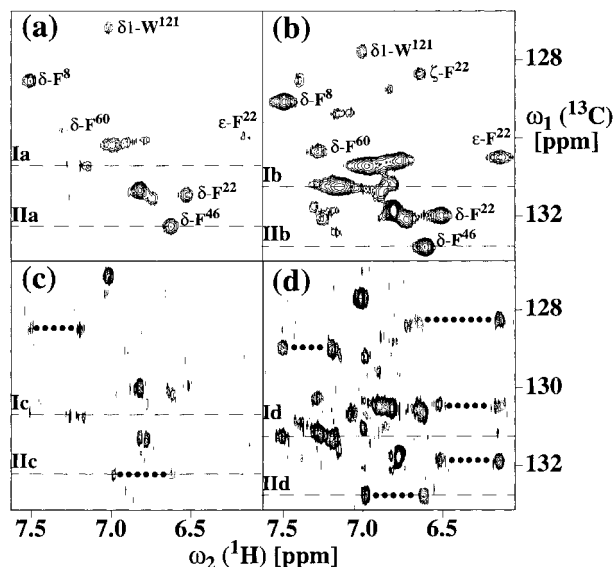


**Figure 2.** Comparison of two direct and two relayed  $^1\text{H}$ - $^{13}\text{C}$  correlation experiments performed with uniformly  $^{13}\text{C}$ -labeled cyclophilin A<sup>15</sup> in  $^2\text{H}_2\text{O}$  solution (protein concentration 1 mM, pD = 6.5, 10 °C) on a Bruker DRX-750 spectrometer. Contour plots of a spectral region that contains resonances of phenylalanyl residues is shown. (a) 2D ct- $^{13}\text{C}$ , $^1\text{H}$ -COSY.<sup>9</sup> (b) 2D ct-TROSY- $^{13}\text{C}$ , $^1\text{H}$ -COSY spectrum recorded using the pulse scheme of Figure 1a with insertion of Figure 1c. (c) 2D ct-(H)C(C)H-COSY.<sup>10</sup> (d) 2D ct-TROSY-(H)C(C)H-COSY spectrum recorded using the pulse scheme of Figure 1b with  $t_2 = 0$  and insertion of Figure 1c. The spectra a and b were recorded with 2048 ( $t_2$ )\*70 ( $t_1$ ) complex points, and c and d with 2048 ( $t_2$ )\*58 ( $t_1$ ) complex points, which resulted in measurement times of 7.5 h each for a and b, and 5.4 h for c and d. The spectra were processed with the program PROSA.<sup>21</sup> Chemical shifts relative to DSS are indicated in ppm in both dimensions. Corresponding peak positions in the  $^{13}\text{C}$  dimension of the spectra a and b, and c and d, respectively, differ by about 80 Hz, since the latter were obtained without proton decoupling during  $t_1$  and only one multiplet component is retained (see text). The dashed lines identify the locations of the cross sections along  $\omega_2$  that are shown in Figure 3. In a and b, the assignments of selected cross-peaks are indicated, and in c and d, the dotted horizontal lines indicate three-bond  $^1\text{H}$ - $^{13}\text{C}$  connectivities in the aromatic rings.

peaks in the  $\omega_1$  and  $\omega_2$  dimensions, respectively. The corresponding cosine-modulated signal in the  $\omega_1$  dimension is obtained with simultaneous incrementation of the phases  $\psi_1$  and  $\psi_2$  by  $90^\circ$ , and the sine-modulated signal in the  $\omega_2$  dimension results from incrementation of the phase  $\psi_3$  by  $90^\circ$ .

## Results

The potential of the TROSY approach for NMR experiments with aromatic spin systems in uniformly  $^{13}\text{C}$ -labeled proteins is first illustrated by comparison of the use of 2D ct-TROSY- $^{13}\text{C}$ , $^1\text{H}$ -COSY (Figure 1a) and ct- $^{13}\text{C}$ , $^1\text{H}$ -COSY<sup>9</sup> to correlate the  $^1\text{H}$  and  $^{13}\text{C}$  resonances of aromatic  $^{13}\text{C}$ - $^1\text{H}$  moieties. The key difference between the two experiments is that in TROSY the evolution of the  $IS$  spin system due to the  $^1J_{IS}$  scalar coupling is not refocused during  $t_1$ , which preserves the differences in DD-CSA interference for the individual multiplet components during this period. A small region from the  $^1\text{H}$ - $^{13}\text{C}$  correlation spectra that contains resonances of aromatic groups of the uniformly  $^{13}\text{C}$ -labeled 18 kDa protein cyclophilin A is compared in Figure 2a,b. The spectra were measured at 10 °C, where the correlation time for cyclophilin A was estimated to be  $\tau_c = 16$  ns, using the experimental value of  $\tau_c = 8$  ns measured at

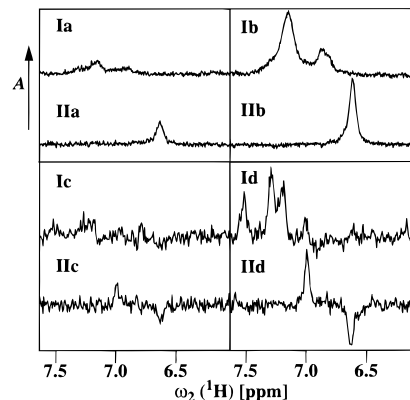


**Figure 3.** Cross sections through the spectra of Figure 2. The numbering Ia, IIa, etc. identifies the cross sections along the corresponding dashed lines in Figure 2. Resonance intensities, A, are plotted versus the  $^1\text{H}$  chemical shift.

26 °C<sup>15</sup> and the temperature dependence of the viscosity of the aqueous solvent. This correlation time corresponds to that of a spherical 30 kDa protein in  $\text{H}_2\text{O}$  at 30 °C. In the TROSY spectrum (Figure 2b) only the downfield component of the  $^{13}\text{C}$  doublets is observed, so that the peak positions along  $\omega_1$  differ from those observed for the same C-H fragment in Figure 2a by about 80 Hz. All the peaks are more intense in Figure 2b, and a number of signals can be identified in the 2D ct-TROSY- $^{13}\text{C}$ , $^1\text{H}$ -COSY spectrum (Figure 2b) that are completely obscured by noise in the conventional experiment (Figure 2a). A quantitative comparison of the relative sensitivity of the two experiments can be obtained from cross sections taken along the  $\omega_2$  dimension (Figure 3). On average, a 6-fold signal-to-noise enhancement was obtained for the TROSY-type experiment. For the individual peaks the enhancement varies from 4 to 10, which reflects different local mobility of the individual aromatic rings. The largest enhancements were obtained for the aromatic rings in the core of the protein, which have the shortest transverse  $^{13}\text{C}$  relaxation times.

The experimental scheme of Figure 1b extends the TROSY approach to correlate the  $^1\text{H}$  and  $^{13}\text{C}$  resonances of a given  $^{13}\text{C}$ - $^1\text{H}$  moiety with the resonances of the directly bound  $^{13}\text{C}$ - $^1\text{H}$  fragments. This experiment enables  $^1\text{H}$  and  $^{13}\text{C}$  resonance assignment for complete aromatic spin systems in uniformly  $^{13}\text{C}$ -labeled proteins. Figure 2d shows the same spectral region as in Figure 2b from a 2D ct-TROSY-(H)C(C)H-COSY spectrum recorded using the experimental scheme of Figure 1b with  $t_2 = 0$ . In this spectrum each aromatic  $^{13}\text{C}$  resonance is correlated on one hand by negative peaks with the resonance of the directly attached proton, and by positive peaks with the resonances of one or two protons separated by two bonds. A comparison with the spectrum in Figure 2c, which was measured with the corresponding conventional experimental scheme,<sup>10</sup> demonstrates that for both the direct peaks and the relay peaks the amplitudes are enhanced by application of TROSY. The sensitivity improvement achieved with the experiment of Figure 1b is similar to that of the direct correlation experiment of Figure 1a, i.e., by a factor of 4–10 for individual lines, as can be estimated from a comparison of the cross sections taken along the  $\omega_2$  dimension (Figure 3c,d). For example, for Phe 22, which is located in the core of the protein and has short  $^{13}\text{C}$  transverse relaxation times, the connectivities identified in Figure 2d (three dotted lines on the right), are not visible in Figure 2c.

(15) Ottiger, M.; Zerbe, O.; Güntert, P.; Wüthrich, K. *J. Mol. Biol.* **1997**, *272*, 64–81.

(16) London, R. E. *J. Magn. Reson.* **1990**, *86*, 410–415.

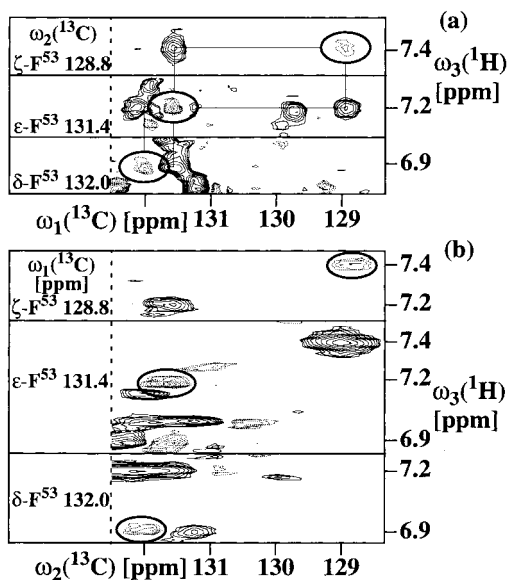


**Figure 4.** 3D ct-TROSY-(H)CCH-COSY experiment recorded with the same sample of cyclophilin A as in Figure 2 on a Bruker DRX-750 spectrometer using the experimental scheme of Figure 1b with insertion of Figure 1c.  $58(t_1) \times 32(t_2) \times 1024(t_3)$  complex points were accumulated, yielding  $t_{1\max} = 11.6$  ms,  $t_{2\max} = 4.4$  ms, and  $t_{3\max} = 102.4$  ms. Sixteen scans per increment were acquired, resulting in a measuring time of 34 h. Prior to Fourier transformation, the size of data matrix was 2-fold extended by linear prediction along  $t_1$  and  $t_2$ . The spectra were processed with the program PROSA.<sup>21</sup> Contour plots of (a)  $[\omega_1(^{13}\text{C}), \omega_3(^1\text{H})]$  strips and (b)  $[\omega_2(^{13}\text{C}), \omega_3(^1\text{H})]$  strips are shown. The strips were taken at the aromatic  $^{13}\text{C}$  chemical shifts of Phe 53, in a along  $\omega_2$ , and in b along  $\omega_1$ . The direct  $^{13}\text{C}$ - $^1\text{H}$  cross-peaks are circled, and in a direct peaks and their corresponding relay peaks are connected with thin lines, thus outlining the identification of the complete aromatic spin system of Phe 53.

For larger proteins the often rather small spectral dispersion of the  $^1\text{H}$  and  $^{13}\text{C}$  resonances in aromatic rings can complicate the resonance assignment. To overcome such limitations the ct-TROSY-(H)C(C)H-COSY spectrum can be resolved in a second carbon dimension, using the 3D ct-TROSY-(H)CCH-COSY scheme of Figure 1b. In this experiment the chemical shift evolution of two neighboring aromatic  $^{13}\text{C}$  spins is recorded in the two indirectly detected spectral dimensions,  $\omega_1$  and  $\omega_2$ . Figure 4a shows contour plots of  $[\omega_1(^{13}\text{C}), \omega_3(^1\text{H})]$  strips from a 3D ct-TROSY-(H)CCH-COSY experiment measured with uniformly  $^{13}\text{C}$ -labeled cyclophilin A, which identify the aromatic spin system of Phe 53. Because the different signs of the direct peaks and the relay cross-peaks may lead to cancellation when such peaks are located in close proximity, it may be helpful to inspect also the  $[\omega_2(^{13}\text{C}), \omega_3(^1\text{H})]$  strips (Figure 4b), where corresponding direct peaks and relay peaks are observed at different proton chemical shifts. The probability of mutual cancellation of positive and negative peaks in crowded spectral regions can be further reduced, either in the 3D or 2D versions of the experiment, through suppression of the direct correlation peaks relative to the relay peaks. This is achieved by choosing the period  $T_a$  shorter than  $3/(4^1J_{\text{CC}})$  and  $T_b$  correspondingly longer than  $1/(4^1J_{\text{CC}})$ , which obviously represents a compromise with regard to obtaining maximal sensitivity. Another technical detail of the 3D experiment of Figure 1b contributes to optimal sensitivity: Both carbon-carbon polarization transfer steps are combined with the recording of the carbon chemical shifts, so that the total time period with carbon magnetization in the transverse plane is not increased when compared to the corresponding 2D experiment. The third spectral dimension is

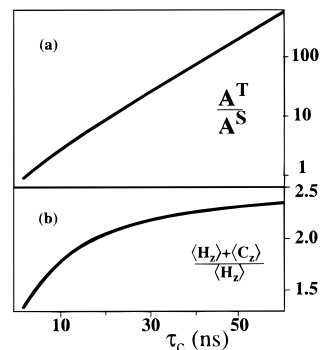


**Figure 5.** Origins of the sensitivity enhancement observed for the 2D ct-TROSY- $^{13}\text{C}$ ,  $^1\text{H}$ -COSY experiment (Figures 2 and 3). (a) Logarithmic plot of the ratio of the calculated 2D correlation peak amplitudes in the TROSY-type experiment ( $A^T$ ) and the standard 2D ct- $^{13}\text{C}$ ,  $^1\text{H}$ -COSY experiment ( $A^S$ ) versus the isotropic rotational correlation time,  $\tau_c$ . The steady-state magnetizations,  $\langle H_z \rangle$  and  $\langle C_z \rangle$ , were estimated using eqs 22–30 in the paper by Goldman (1984).<sup>8</sup> Six  $^1\text{H}$  spins were placed at 0.25 nm from the  $^1\text{H}$  spin of the  $^{13}\text{C}$ - $^1\text{H}$  moiety to account for the influence of long-range DD interactions on  $T_1$  ( $^1\text{H}$ ). In the calculation the following parameters were used:  $^{13}\text{C}$  constant-time delay,  $T = 1/J_{\text{CC}} = 17.6$  ms; delay between successive recordings = 1 s;  $\omega_S = 1.18 \times 10^9$  rad  $\text{s}^{-1}$  at the magnetic field strength corresponding to a  $^1\text{H}$  resonance frequency of 750 MHz;  $J(\omega) = 0.4(\tau_c/(1+(\tau_c\omega)^2))$ ;  $^{13}\text{C}$ - $^1\text{H}$  distance,  $r_{\text{IS}} = 0.109$  nm;  $\Delta_1 = \sigma_{33} - \sigma_{11} = -210$  ppm;  $\Delta_2 = \sigma_{22} - \sigma_{11} = -76$  ppm;  $\Phi_1 = 90^\circ$ ;  $\Phi_2 = 90^\circ$ ;  $\gamma_I = 2.67 \times 10^8$  rad  $\text{s}^{-1} \text{T}^{-1}$ ;  $\gamma_S = 6.73 \times 10^7$  rad  $\text{s}^{-1} \text{T}^{-1}$ ;  $\hbar = 1.05 \times 10^{-34}$  J s. (b) Plot of the ratio of two alternative choices for the steady-state magnetization that can be used in TROSY,  $\langle H_z \rangle$  and  $\langle H_z \rangle + \langle C_z \rangle$ , vs  $\tau_c$ . The relaxation rates of  $\langle H_z \rangle$  and  $\langle C_z \rangle$  were estimated using eqs 22–30 in the paper by Goldman (1984).<sup>8</sup>

thus obtained without increase of the number of delays, which contributes to minimizing losses of signal due to transverse  $^{13}\text{C}$  relaxation.

## Discussion

Despite the now quite generally available uniform  $^{13}\text{C}$ -labeling and an impressive repertoire of NMR experiments, the assignment of aromatic spin systems remains a challenging task for larger proteins because of fast transverse  $^{13}\text{C}$  relaxation and typically very limited  $^1\text{H}$  and  $^{13}\text{C}$  chemical shift dispersion. Additional difficulties may arise for individual rings of phenylalanine and tyrosine because of “ring flipping”<sup>23</sup> at slow or intermediate frequencies on the chemical shift time scales. In the following we investigate how these different limiting factors are manifested in TROSY-type NMR experiments, also in comparison with alternative experimental approaches.

The major advance with the TROSY approach is the improved sensitivity for detection of aromatic  $^{13}\text{C}$ - $^1\text{H}$  correlations (Figures 2 and 3). To estimate the sensitivity enhancement for 2D ct-TROSY- $^{13}\text{C}$ ,  $^1\text{H}$ -COSY relative to the corresponding standard experiment,<sup>9</sup> Figure 5a presents the ratio of corresponding cross-peak amplitudes in these two experiments,  $A^T$  and  $A^S$ , vs the effective isotropic correlation time for the  $^{13}\text{C}$ - $^1\text{H}$  bond,  $\tau_c$ , calculated with

$$\frac{A^T}{A^S} = \frac{1}{2} \frac{\langle H_z \rangle + \langle C_z \rangle}{\langle H_z \rangle} \exp(-\eta T) \quad (14)$$

where  $\langle H_z \rangle$  and  $\langle C_z \rangle$  are the steady-state magnetizations for  $^1\text{H}$  and  $^{13}\text{C}$ ,  $\eta$  is the  $^{13}\text{C}$  DD-CSA interference term given by eq 2, and  $T$  is the  $^{13}\text{C}$  constant-time delay. The parameters used for the calculation of Figure 5a are listed in the figure caption. The steady-state magnetizations  $\langle H_z \rangle$  and  $\langle C_z \rangle$  were estimated

using eqs 22–30 in the paper by Goldman (1984).<sup>8</sup> Six  $^1\text{H}$  spins are placed at 0.25 nm from the  $^1\text{H}$  spin of the  $^{13}\text{C}$ – $^1\text{H}$  moiety to account for the influence of long-range DD interactions on  $T_1(^1\text{H})$ . Since the  $^{13}\text{C}$  chemical shifts are recorded during a constant-time period, the ratio of the cross-peak amplitudes grows exponentially with  $\tau_c$  and hence with the protein size (note the logarithmic scale in Figure 5a). For  $\tau_c$  around 15 ns, an enhancement factor of 7 is predicted, which corresponds closely to the experimental data obtained with cyclophilin A at 10° C (Figure 3). Overall, Figure 5a predicts that TROSY-type experiments will show superior sensitivity for proteins of all sizes, when compared to the corresponding conventional experiments.

Part of the signal enhancement for the TROSY-type experiments shown in Figure 5a is due to the use of the steady-state  $^{13}\text{C}$  magnetization (eq 3). In Figure 5b, which compares the relative contributions of the steady-state  $^1\text{H}$  and  $^{13}\text{C}$  magnetizations to the observed signal (see eq 14), this effect is considered separately. For  $\tau_c$  values in the range 10–60 ns, the two magnetizations are predicted to contribute comparably to the resulting signal, which also opens the possibility to achieve suppression of the fast relaxing component of the  $^{13}\text{C}$  doublet by combined use of the  $^1\text{H}$  and  $^{13}\text{C}$  steady-state magnetizations (see Figure 6).

To verify the predictions of Figure 5 about the relative contributions of the steady-state  $^1\text{H}$  and  $^{13}\text{C}$  magnetizations to the observed signal, the experimental scheme of Figure 1a was used with the 14 kDa C-terminal domain of the human prion protein, hPrP(121–231). For this small protein at 20 °C both components of the  $^{13}\text{C}$  doublet can be observed along the  $\omega_1$  dimension in the 2D ct-TROSY- $^{13}\text{C}$ , $^1\text{H}$ -COSY spectra (Figure 6). In the first three of these test measurements (Figure 6a–c), the element of Figure 1c<sup>17</sup> was used without application of the pulse  $\psi_c$ , so that the phase of one doublet component is shifted relative to the other one by 90° (see eqs 7 and 8). The cross sections a and b in Figure 6 were taken from spectra measured with dephasing of either the  $^{13}\text{C}$  or the  $^1\text{H}$  steady-state magnetization before the start of the pulse sequence. Figure 6c is taken from a spectrum recorded without dephasing of either of the steady-state magnetizations, which results in nearly complete suppression of the higher field-shifted multiplet component. The combined use of the two steady-state magnetizations also resulted in 2-fold enhancement of the amplitude of the observed component (compare Figure 6c with Figure 6, a or b). The nearly complete cancellation of the unwanted component in Figure 6c is not noticeably improved by additional application of the pulse  $\psi_c$  (Figure 6d), showing that with the use of  $^{13}\text{C}$  steady-state magnetization the element of Figure 1c can be safely omitted for all but the smallest proteins, since the unwanted component of the  $^{13}\text{C}$  doublet is attenuated beyond detection. The  $^{13}\text{C}$  steady-state magnetization, which was recently also constructively used for obtaining axial peaks in reduced-dimensionality triple resonance spectra,<sup>18</sup> thus contributes here directly to improved sensitivity of the desired multiplet component.

An important practical consideration is the range of resonance frequencies for which the TROSY approach yields the aforementioned advantages of improved sensitivity. Maximal  $T_2$  suppression for one component of the  $^{13}\text{C}$  doublet is achieved at a  $^1\text{H}$  frequency near 600 MHz, and values near this maximum

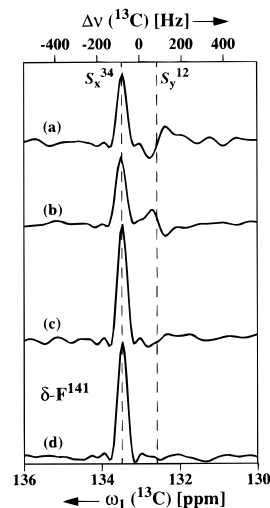


**Figure 6.** Combined use of  $^1\text{H}$  and  $^{13}\text{C}$  steady-state magnetization for signal enhancement and suppression of unwanted peaks. The figure shows 2D ct-TROSY- $^{13}\text{C}$ , $^1\text{H}$ -COSY spectra recorded with the uniformly  $^{13}\text{C}$ , $^{15}\text{N}$ -labeled hPrP(121–231) in  $^2\text{H}_2\text{O}$  solution (protein concentration 1 mM, pD = 4.5, 20 °C) on a Bruker DRX-750 spectrometer using the pulse sequence of Figure 1a with the insertion of Figure 1c. Cross sections along  $\omega_1(^{13}\text{C})$  are shown which comprise the resonances of the  $^{13}\text{C}$  doublet of the aromatic  $^{13}\text{C}$ – $^1\text{H}$  moiety of Phe141. (a) The steady-state  $^{13}\text{C}$  magnetization was dephased before the first 90° proton pulse by application of a high-power spin-lock pulse for 4 ms on the carbon channel followed by a 1-ms PFG of 30 G/cm. The signals of the two  $^{13}\text{C}$  multiplet components,  $S_x^{34}$  and  $S_y^{12}$ , have a phase difference of 90°. (b) The steady-state  $^1\text{H}$  magnetization was similarly dephased by application of a 4 ms spin-lock pulse on the proton channel. In c and d, neither of the steady-state proton or carbon magnetizations was dephased so that both contributed to the observed signal. In a, b, and c the element of Figure 1c was applied without executing the pulse  $\psi_c$ , so that both components of the  $^{13}\text{C}$  doublet were retained. Otherwise the total recording time and the experimental parameters were identical in all four experiments, so that a comparison of c and d offers an illustration of the impact of the pulse  $\psi_c$  (Figure 1). Chemical shifts relative to ppm (bottom) and shifts in Hz relative to the center of the  $^{13}\text{C}$  doublet (top) are indicated. The resonance positions of the two multiplet components are indicated by vertical dashed lines.

are achieved over the range from 500 to 800 MHz, i.e., the entire frequency range that is currently of interest for high-resolution NMR with proteins. This compares favorably with the situation for  $^{15}\text{N}$ – $^1\text{H}$  moieties in proteins, where maximal  $T_2$  suppression is obtained at a  $^1\text{H}$  frequency near 1 GHz.<sup>2</sup> The significance of each contributing relaxation mechanism can be estimated using eqs 1 and 2. For an aromatic spin system at a  $^1\text{H}$  resonance frequency of 750 MHz the magnitudes of the interactions underlying the different individual relaxation mechanisms are  $p = 2.83 \times 10^9$  (rad/s)<sup>2</sup>,  $\delta_S = 2.64 \times 10^9$  (rad/s)<sup>2</sup> and  $K_1 + K_2 = 4.25 \times 10^9$  (rad/s)<sup>2</sup>. This results in a residual magnitude of the overall interaction of  $1.22 \times 10^9$  (rad/s)<sup>2</sup> in the TROSY experiment, and  $5.47 \times 10^9$  (rad/s)<sup>2</sup> in conventional ct- $^{13}\text{C}$ , $^1\text{H}$ -COSY.<sup>9</sup> These numbers show that the DD and CSA autorelaxation terms of a proton-bound aromatic carbon-13 spin are compensated in the extent of about 80% by the cross-correlation terms, where the incomplete compensation is due to the fact that the chemical shift tensor for aromatic carbons deviates from axial symmetry.<sup>12</sup> Another contribution to the residual relaxation of  $^{13}\text{C}$ , in the extent of about  $1.0 \times 10^9$  (rad/s)<sup>2</sup>, comes from homonuclear proton–proton longitudinal relaxation.<sup>2</sup> This contribution of the longitudinal relaxation to the transverse relaxation of  $^{13}\text{C}$  in aromatic  $^{13}\text{C}$ – $^1\text{H}$  groups is due to DD interactions with remote hydrogen atoms and hence

(17) Meissner, A.; Duus, J.Ø.; Sørensen, O. W. *J. Biomol. NMR* **1997**, *10*, 89–94. Sørensen, M. D.; Meissner, A.; Sørensen, O. W. *J. Biomol. NMR* **1997**, *10*, 181–186.

(18) Szyperski, T.; Braun, D.; Banecki, B.; Wüthrich, K. *J. Am. Chem. Soc.* **1996**, *118*, 8146–8147.

is nearly independent of the frequency. For studies of larger proteins, this relaxation pathway can be partially suppressed by reverse  $^1\text{H}$ -labeling of the aromatic residues in otherwise perdeuterated proteins.<sup>5</sup>

Finally, line broadening for the aromatic rings of the Phe and Tyr due to slow "ring flipping"<sup>3,19</sup> may prevent observation of individual aromatic spin systems also by TROSY-type experiments. It should, however, be considered that due to the larger gyromagnetic ratio and the generally larger chemical shift

---

(19) Wüthrich, K.; Wagner, G. *FEBS Lett.* **1975**, *50*, 265–268. Wüthrich, K.; Wagner, G. *Trends Biochem. Sci.* **1978**, *3*, 227–230. Wüthrich, K.; Wagner, G. *Nature* **1978**, *275*, 247–248. Nall B. T.; Zuniga, E. H. *Biochemistry* **1990**, *29*, 7576–7584. Lian, C.; Le, H.; Montez, B.; Patterson, J.; Harrell, S.; Laws, D.; Matsumura, I.; Pearson, J.; Oldfield, E. *Biochemistry* **1994**, *33*, 5238–5245.

(20) Marion, D.; Ikura, M.; Tschudin, R.; Bax, A. *J. Magn. Reson.* **1989**, *39*, 163–168.

dispersion, the aromatic  $^1\text{H}$  resonances are intrinsically more sensitive to the flipping motions than the  $^{13}\text{C}$  resonances. As a result, use of HMQC-type NMR experiments, where both  $^1\text{H}$  and  $^{13}\text{C}$  nuclei evolve in the transverse plane, is less favorable in critical situations than the single quantum coherence scheme used in the TROSY approach, where the evolution time of transverse proton magnetization is minimized.

**Acknowledgment.** Financial support was obtained from the Schweizerischer Nationalfonds (project 31.49047.96). We thank Dr. M. Ottiger and Dr. R. Zahn for providing us with the samples of cyclophilin A and hPrP(121–231).

JA980742G

---

(21) Güntert, P.; Dötsch, V.; Wider, G.; Wüthrich, K. *J. Biomol. NMR* **1992**, *2*, 619–629.